symmetry

MDPI

Article

An Adaptive Moving Mesh Method for Solving Optimal Control Problems in Viscous Incompressible Fluid

Junxiang Lu [1,*,†], Hong Xue [1,†] and Xianbao Duan [2,†]

1 Department of Mathematics of School of Science, Xi'an Polytechnic University, Xi'an 710048, China; xuehonghong@sohu.com
2 Department of Mathematics of School of Science, Xi'an University of Technology, Xi'an 710049, China; xianbaoduan@hotmail.com
* Correspondence: jun-xianglu@163.com; Tel.: +86-1357-211-2415
† These authors contributed equally to this work.

Abstract: An adaptive moving mesh method for optimal control problems in viscous incompressible fluid is proposed with the incompressible Navier–Stokes system used to describe the motion of the fluid. The moving distance of nodes in the adopted mesh moving strategy is found by solving a diffusion equation with source terms, and an algorithm that fully considers the characteristics of the control problem is given with symmetry reduction to the incompressible Navier–Stokes equations. Numerical examples are provided to show that the proposed algorithm can solve the optimal control problem stably and efficiently on the premise of ensuring high precision.

Keywords: moving mesh method; optimal control problem; finite element method; Navier–Stokes equation

check for updates

Citation: Lu, J.; Xue, H.; Duan, X. An Adaptive Moving Mesh Method for Solving Optimal Control Problems in Viscous Incompressible Fluid. *Symmetry* **2022**, *14*, 707. https://doi.org/10.3390/sym14040707

Academic Editors: Alexander Zaslavski and Mikhail Sheremet

Received: 8 March 2022
Accepted: 24 March 2022
Published: 31 March 2022

1. Introduction

The optimal control problems constrained by PDEs play an increasingly important role in engineering and have attracted widespread attention from many scholars. These problems cover various fields, such as feedback control, the control of fluid flow and optimal shape design [1–3]. The research on numerical methods for these problems has been an active area in recent decades. To approximate the solutions of control problems, the FEM (finite element method) proves to be a powerful method and has been used as the main method in dealing with numerical analysis for optimal control problems [4–7].

Efficient numerical solutions to optimal control problems constrained by PDEs involve many fields, and this is particularly true for fluid dynamics problems. Within the context of optimal control problems, the flow control is crucial for various engineering applications [8–10]. Therefore, flow control has become an increasingly active field and has undergone much progress in its theoretical aspects [11–17].

From the perspective of numerical solutions only, effective discretization schemes for the non-linear state equations are quite challenging, especially when considering practical industrial application problems. The finite element method is undoubtedly the most appropriate tool to compute the flow control problems. Recently, there has been extensive research in theoretical analysis and numerical approximation of the fluid dynamics equations in the scientific literature [18,19].

Researchers have developed some results of the FEM for flow control problems [16,20]. There is also some research on state-constrained control problems constrained by fluid dynamics equations [13,14]. In [11], Abergel and Temam studied first order optimality conditions and gave a gradient algorithm. Wang obtained some theoretical results of state-constrained optimal control problems for 3-D instantaneous fluid flow [21]. Gunzburger, Hou and Svobodny first studied the FEM for optimal control problems about steady-state fluid flow in [15]. Similar problems were discussed in [16]. However, most of those works were based on a uniform mesh, which leads to a time-consuming procedure.

Hydrodynamic problems generally involve interface tracking, shock waves, singularities of solutions, phase changes, and high vorticity or complex areas. When numerically solving these problems, there is usually some form of spatial mesh, and mesh-dependent methods were adopted. However, these methods are not so efficient when the solution involves a large change in the local area [21,22]. It should be noted that there are usually regularities in optimal control problems, and the singularities likely distribute to different positions, which means that the uniform triangulation strategy may be inefficient. The adaptive mesh method is more efficient to deal with in that case. This enables us to use as few meshes as possible to solve the state equations using the adaptive mesh method [23–25].

Adaptive FEM, which was proposed by the pioneering work in [26], is becoming an active field in scientific and engineer computations for its high efficiency among various kinds of finite element methods.To achieve a higher accuracy and minimize the computational work as much as possible, adaptive FEM is undoubtedly a particularly appropriate finite element tool in solving PDEs [27–32].

The adaptive mesh method usually divides the working domain uniformly first, and then adds or deletes mesh nodes to locally refine or coarsen according to a posteriori error estimation. This is the basic idea of the h-method, and many commercial software programs are also based on this strategy. Another method is the p-method, which increases the number of interpolation polynomials to improve the accuracy of the solution, most commonly in the FEM.

The p-method can be combined with the h-method, and the hp-method [33,34] is obtained through a posteriori error estimation. The hp-method has been developed to relative maturity; however, the implementation of this method is quite complicated, because a posteriori error estimation depends heavily on certain assumptions of the solution, and these assumptions may be difficult to obtain for many nonlinear problems. This work considers another adaptive mesh method—namely, the r-method (moving mesh method).

Although the r-method is not as widely used as the h- or p-methods, it has also been used in many fields and has achieved good results [35–40]. Although the r-method has many promising features in solving complex problems, there are more problems that need to be solved compared to the h-method and the p-method. The idea of the r-method is to start with a given initial mesh, then move the nodes according to the characteristics of the solution or region and keep the mesh topology and the number of nodes unchanged during the solution process.

In the end, the nodes are concentrated in local areas, which usually have more drastic solution changes or more complex geometric shapes. Therefore, the moving mesh method could save computational effort while the same accuracy is achieved. These techniques can be widely used in physics, mechanics, engineering and other fields and are applied to various problems and algorithm selection, including solving various dynamic equations, detonation simulation and other problems.

In order to solve the optimal control problems constrained by PDEs, we integrate the sensitivity analysis results with the moving mesh strategy and take the incompressible viscous fluid as an example. The structure of this study is the following: In Section 2, the optimal control problem with a Navier–Stokes equation as the state constraint is given, and sensitivity analysis results are obtained by the adjoint method. Section 3 presents an improved moving mesh method. Section 4 presents an adaptive moving mesh method to solve the optimal control problem, and a verification example is provided. A brief summary is given in the last section.

2. Optimal Control Problem and Sensitivity Analysis

We assume that $\mathcal{U}$ and $\mathcal{Y}$ are two Hilbert spaces, and our goal is to find the minimum value of the functional

$$\mathcal{J} : \mathcal{Y} \times \mathcal{U} \to \mathbb{R} \tag{1}$$

constrained by

$$\mathcal{E}(y, u) = 0, \tag{2}$$

where $y \in \mathcal{Y}$ and $u \in \mathcal{U}$ represent the state variable and the control variable, respectively. $\mathcal{Y}$ depends on u—that is, $y = y(u)$. Usually, there is $y \in \mathcal{Y}_{ad} \subset \mathcal{Y}$, $u \in \mathcal{U}_{ad} \subset \mathcal{U}$. $\mathcal{Y}_{ad}$ and $\mathcal{U}_{ad}$ are admissible spaces. For steady problems, constraints (2) are PDEs with corresponding boundary conditions. For the Navier–Stokes equations, the constraints (2) are:

$$\begin{cases} -\nu\Delta y + y\cdot\nabla y + \nabla p &= f + u_D, & \text{in } \Omega, \\ -\operatorname{div} y &= 0, & \text{in } \Omega, \\ y &= g, & \text{on } \Gamma_d, \\ y &= u_B, & \text{on } \Gamma_c, \\ \nu\frac{\partial y}{\partial n} &= p_n, & \text{on } \Gamma_n, \end{cases} \tag{3}$$

where $\Omega \subset \mathbb{R}^d, d \in \{2,3\}$ is the working area. The constraint variable $y := (y, p)$ and the speed $y = (y_i)_{i=1}^d$ and pressure p are unknown. f is the volume force. ν is the viscosity coefficient. g is a known function. The functions u_D and u_B are control variables. Γ_d and Γ_c are both Dirichlet boundary conditions for speed, which can be homogeneous or non-homogeneous; however, the meaning is different at the boundary. Non-homogeneous on Γ_d generally means inflow or outflow, and homogeneous means that there is no slip condition on the solid wall, while on the boundary Γ_c, non-homogeneous means the value of the control variable. n represents the unit normal vector. The boundary of the region is $\partial\Omega := \Gamma = \overline{\Gamma_d \cup \Gamma_c \cup \Gamma_n}$.

The typical objective functional $\mathfrak{J}$ in the optimal control problem is:

$$\mathcal{J}(y,u) = \frac{1}{2}\int_{\Omega_c} |y - y_d|^2 dx + \frac{\alpha}{2}\|u\|^2_{\Omega_c}, \tag{4}$$

Equation (4) means the distance between the state Equation (2) to a given goal or expectation of the state y_d. In order for the problem to be well posed, we also include the control in the cost functional, together with a Tikhonov regularization parameter α, which is usually chosen a priori, and the control volume is $\Omega_c \subset \Omega$. Equation (4) means the distance between the state Equation (2) to a given goal or expectation of the state y_d. Similarly, we can define this distance as the target functional only on the boundary $\partial\Omega$ or part of it.

Let $V := H^1(\Omega)^d$, which means that the function itself and its first derivative belong to the Sobolev space formed by the vector value function of $L^2(\Omega)$. Let

$$\tilde{\mathcal{Y}} := \left\{ \tilde{y} \in V = H^1(\Omega)^d : \tilde{y}|_{\Sigma_d \cup \Sigma_c} = 0 \right\},$$

and

$$P := L_0^2(\Omega) = \left\{ p \in L^2(\Omega) : \int_\Omega p dx = 0 \right\}.$$

Then, the weak form of the Navier–Stokes problem (3) is:

$$\begin{cases} \nu(\nabla y, \nabla\tilde{y})_\Omega + (y\cdot\nabla y, \tilde{y})_\Omega & \\ -(p, \operatorname{div}\tilde{y})_\Omega - (f + u_D, \tilde{y})_\Omega = 0, & \forall \tilde{y} \in \tilde{\mathcal{Y}}, \\ -(\operatorname{div} y, q)_\Omega = 0, & \forall q \in P, \\ y = g, & \text{on } \Sigma_d, \\ y = u_B, & \text{on } \Sigma_c, \end{cases} \tag{5}$$

where $(\cdot,\cdot)_\Omega$ represents the inner product of L^2.

Let the area $\Omega_h \subset \Omega$ be a triangulation with h as the parameter $\mathcal{T}_h$, $\tilde{\mathcal{Y}}_h \subset \tilde{\mathcal{Y}}$ and $P_h \subset P$ are two finite element spaces. Then, the finite element solution of problem (5) is:

Find $(\tilde{y}_h, p_h) \in \tilde{\mathcal{Y}}_h \times P_h$, such that

$$\begin{cases} \nu(\nabla y_h, \nabla \tilde{y}_h) + (y_h \cdot \nabla y_h, \tilde{y}_h) \\ \qquad -(p_h, \nabla \cdot \tilde{y}_h) = (f_h, \tilde{y}_h), \quad \forall \tilde{y}_h \in \tilde{\mathcal{Y}}_h, \\ \qquad\qquad (q_h, \nabla \cdot y_h) = 0, \quad \forall q_h \in P_h. \end{cases} \tag{6}$$

Let the Lagrange multiplier $L = (l_1, l_2, l_3, l_4) \in \tilde{\mathcal{Y}} \times P \times L^2(\Gamma_d)^d \times L^2(\Gamma_c)^d$. Using integration by parts, we have

$$\begin{aligned} L(y, u, L) =& \mathcal{J}(y, p, u) + \nu(\nabla y, \nabla l_1)_\Omega + (y \cdot \nabla y, l_1)_\Omega \\ & - (p, \operatorname{div} l_1)_\Omega - (f + u_D, l_1)_\Omega \\ & - (\operatorname{div} y, l_2)_\Omega + (y - g, l_3)_{\Gamma_d} \\ & + (y - u_B, l_4)_{\Gamma_c}. \end{aligned} \tag{7}$$

Deriving the above equation in the direction $(\tilde{y}, q)$, we can obtain the weak form of the adjoint problem:

$$\begin{cases} \nu(\nabla \tilde{y}, \nabla l_1)_\Omega + (y \cdot \nabla \tilde{y} + \tilde{y} \cdot \nabla y, l_1)_\Omega - (\operatorname{div} \tilde{y}, l_2)_\Omega \\ \qquad +(\tilde{y}, l_3)_{\Gamma_d} + (\tilde{y}, l_4)_{\Gamma_c} = -\mathcal{J}_y(y, p, u)\tilde{y}, \forall \tilde{y} \in V, \\ \qquad\qquad -(\operatorname{div} l_1, q)_\Omega = -\mathcal{J}_p(y, p, u)q, \forall q \in P. \end{cases} \tag{8}$$

As $l_1 \in \tilde{\mathcal{Y}}$, then using integration by parts, we have

$$\begin{cases} \nu(\nabla \tilde{y}, \nabla l_1)_\Omega = -(\operatorname{div}(\nu \nabla l_1), \tilde{y})_\Omega \\ \qquad\qquad + \nu(\partial_n l_1, \tilde{y})_{\Gamma_n \cup \Gamma_d \cup \Gamma_c}, \\ -(\operatorname{div} \tilde{y}, l_2)_\Omega = (\nabla l_2, \tilde{y})_\Omega - (l_2 n, \tilde{y})_{\Gamma_n \cup \Gamma_d \cup \Gamma_c}, \\ (y \cdot \nabla \tilde{y}, l_1)_\Omega = -(y \cdot \nabla l_1, \tilde{y})_\Omega + ((y \cdot n) l_1, \tilde{y})_{\Gamma_n}. \end{cases} \tag{9}$$

Let $l := l_1, \tilde{l} := l_2$, the adjoint problem can be written as follows:

$$\begin{cases} -\operatorname{div}(\nu \nabla l) - y \cdot \nabla l + (\nabla y) \cdot l + \nabla \tilde{l} \\ \qquad\qquad = -\mathcal{J}_y(y, p, u), & \text{in } \Omega, \\ -\operatorname{div} l = -\mathcal{J}_p(y, p, u), & \text{in } \Omega, \\ l = 0, & \text{on } \Gamma_d \cup \Gamma_c, \\ \nu \dfrac{\partial l}{\partial n} - \tilde{l} n + (y \cdot n) l = 0, & \text{on } \Gamma_n. \end{cases} \tag{10}$$

Deriving u on both sides of Equation (7), we find:

$$\mathcal{J}_u(y, u_D) = l. \tag{11}$$

Combining the adjoint problem (10), the sensitivity analysis result of the objective function about the control variable can be obtained from (11).

3. Moving Mesh Strategy

In our previous work, the moving mesh strategy was as follows [41]. Assume that the finite element triangulation at time T_i is $\mathcal{T}_i$, and the coordinate of the k-th node is X_k^i, then the coordinate of the k-th node at the moment of T_{i+1} can be obtained by the following relationship:

$$X_k^{i+1} = \gamma \xi X_k^i, \tag{12}$$

where $\gamma \geq 0$ is an adjustable parameter, and ξ is the amount of node movement, which is obtained by solving the following diffusion problem that takes the solution of the Navier–Stokes problem (3) as the source term:

$$\begin{cases} \tilde{\xi}_t - \mu \mathcal{M} \Delta \tilde{\xi} = v, & \text{in } \Omega, \\ \tilde{\xi} = 0, & \text{on } \partial\Omega, \end{cases} \tag{13}$$

where $\mathcal{M}$ is the monitor function and v is the solution of Equation (3).

In the first equation of question (13), the right-hand term v reflects the effect of the fluid required by the Navier–Stokes problem (3) on the movement of the mesh. Although it is usually apt to appear with discontinuities and high vorticity where the flow velocity is large, the change of the solution is not necessarily dramatic. The measure taken in [41] is to introduce the gradient information of the solution in the monitor function. In problem (13), homogeneous Dirichilet boundary conditions forcing nodes could not move on the boundary. In this work, the mesh moving equation is improved as:

$$\begin{cases} \xi_t - \mu \mathcal{M} \Delta \xi = \mathcal{J}_u(y, u_D), & \text{in } \Omega, \\ \dfrac{\partial \xi}{\partial n} = 0, & \text{on } \partial\Omega. \end{cases} \tag{14}$$

In the moving mesh method, the monitor function plays a crucial role. In fact, the selection and construction of the monitor function is critical in the moving mesh method. A good monitor function can improve the accuracy of the solution or reduce the local error. For the Navier–Stokes problem, there are some monitor functions that have been suggested in existing works. For example, the monitor functions adopted in [42] are:

$$G = \sqrt{1 + \alpha_1 [\eta(v_h) / \max \eta(v_h)]^{\alpha_2}}, \tag{15}$$

where $\alpha_1 \in R$, $\alpha_2 > 2$ are adjustable parameters, and $\eta(v_h)$ is the error $|v - v_h|_{1,\Omega}$

$$\eta(v_h) := \sqrt{\sum_{l:\text{inner boundaries}} \int_l [\nabla v) h \cdot n_l] \Big|_l^2 \mathrm{d}l}, \tag{16}$$

$[v]\big|_l = v\big|_{l^-} - v\big|_{l^+}$ is the leap along the boundary l.

For the problems studied in this paper, we use the following monitor functions:

$$\mathcal{M} = \sqrt{1 + \beta_1 |\mathcal{J}_u(y, u_D)| + \beta_2 \mathcal{E}}, \tag{17}$$

where $0 < \beta_1, \beta_2 \in R$ are adjustable parameters—that is, the source term was replaced by the sensitivity analysis result of the objective functional. The numerical example shows that this choice could achieve better results. $\mathcal{E}$ is the residual-type a posteriori error estimation of the Navier–Stokes problem,

$$\mathcal{E} = h_T^2 \|f\|_{L^2(T)}^2 + h_T \|J_h(\partial_n \boldsymbol{u})\|_{L^2(\partial T \cap \Omega)}^2 + h_T \|g - \partial_n \boldsymbol{u}\|_{L^2(\partial T \cap \Gamma_N)}^2, \tag{18}$$

where Γ_N is the Neumann boundary, $h_T = \max \operatorname{diam}(h_E)$ (h_E is the triangle), and $J_h(\cdot)$ denotes the jumps. Assume T_+, T_- have a common side, n_+ and n_- are unit normal vectors accordingly, then:

$$J_h(\partial_n \boldsymbol{u})\big|_E := \nabla \boldsymbol{u}\big|_{T_+} \cdot n_+ + \nabla \boldsymbol{u}\big|_{T_-} \cdot n_-. \tag{19}$$

For more discussion on the a posteriori error estimation of the Navier–Stokes problem, please refer to [43,44].

4. Numerical Algorithm and Numerical Example

4.1. Numerical Algorithm

Based on the results in the previous sections, we give the moving mesh method to solve the optimal control problem constraints by the Navier–Stokes equation as follows:

I Divide the working domain Ω uniformly to obtain the initial triangulation $\mathcal{T}^{(0)}$ and the corresponding coordinates of the node is $X^{(0)}$. Then, solve the Navier–Stokes problem (3) to obtain the solution $v_h^{(0)}, p_h^{(0)}$ and the solution of the adjoint problem (10) $l^{(0)}$. Obtain the value $\mathcal{J}_u^{(0)}(y, u_D)$. Select the appropriate parameters γ, β_1, β_2; given the termination criteria *tol*;.

II If $|\mathcal{J}_u^{(i+1)}(y, u_D) - \mathcal{J}_u^{(i)}(y, u_D)| > tol$, then iterate as follows. Step $i+1$ includes the following items:

- The objective function $\mathcal{M}^{(i+1)}$ is obtained by Equation (17); The mesh move amount $\xi^{(i+1)}$ is obtained by Equation (14); Equation (12) moves the mesh node to $X^{(i+1)}$.
- From $X^{(i+1)}$, we find the new triangulation $\mathcal{T}^{(i+1)}$.
- Solve the Navier–Stokes problem (3) to obtain the solution $v_h^{(i+1)}, p_h^{(i+1)}$ and the solution of the adjoint problem (10) $l^{(i+1)}$. Find the values of $\mathcal{J}_u^{(i+1)}(y, u_D)$. Calculate $|\mathcal{J}_u^{(i+1)}(y, u_D) - \mathcal{J}_u^{(i)}(y, u_D)|$.

4.2. Numerical Example

We consider the classical backstep flow with $\nu = 0.002$ (i.e., $Re = 500$). Assume that $\boldsymbol{u} = (0.25 - (y - 0.5)^2, 0.0)^T$ on the inflow boundary, $\boldsymbol{u}_y = 0$, $p = 0$ on the outflow boundary, and $\boldsymbol{u} = 0$ on the rest of the boundaries. The computational domain of the backstep problem is depicted in Figure 1. The target flow field with $\nu = 1$ is shown in Figure 2.

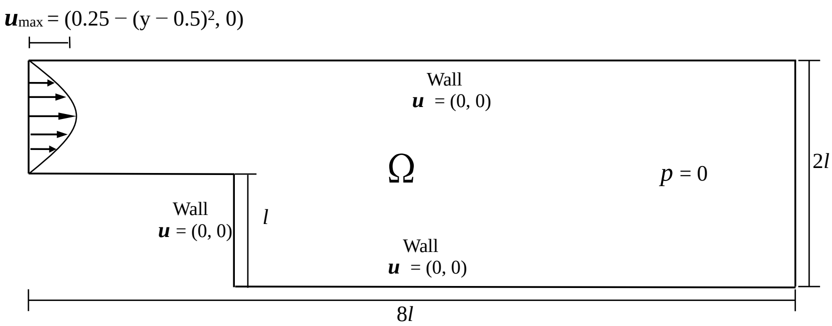

Figure 1. The computational domain of the back-step problem.

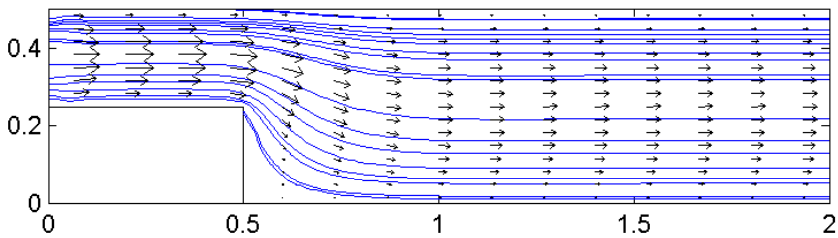

Figure 2. The target flow field.

Figure 3 gives the initial triangulation, and Figure 4 shows the moving mesh produced by the strategy we proposed.

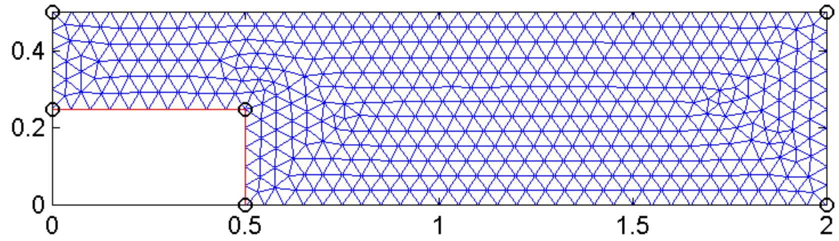

Figure 3. The initial mesh.

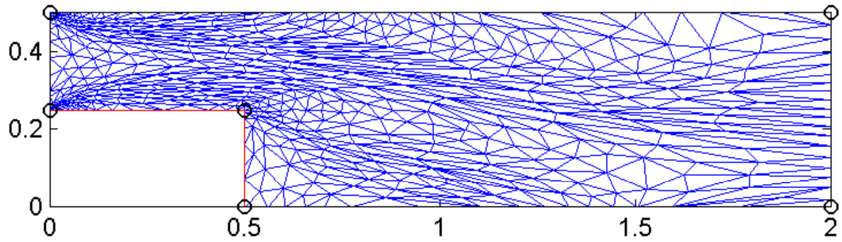

Figure 4. The mesh after moving.

The numerical solution without control is shown in Figure 5, and Figure 6 is the controlled fluid flow.

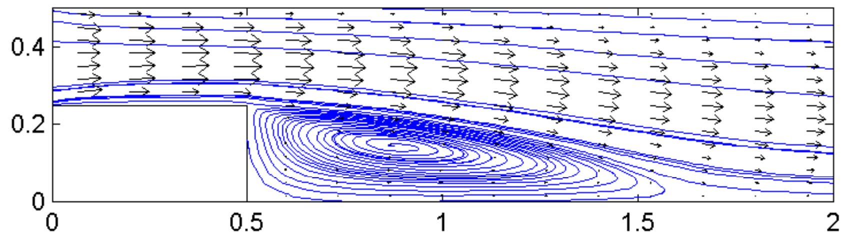

Figure 5. The uncontrolled fluid flow.

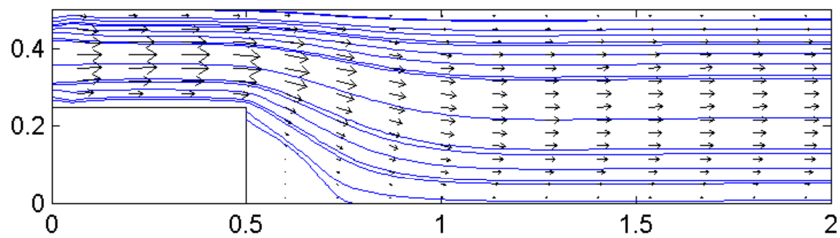

Figure 6. The controlled fluid flow.

The value of the objective function without control is 1.05, while the valued of the objective function after control is 5.2×10^{-4}. This means that the value of the objective function has been reduced to about 0.5%.

It can be seen from the results that the mesh will be automatically focused on the place where the solution change is relatively large. We also solved the problem with uniform triangulation. To achieve the same numerical accuracy, the nodes need to be doubled and the time-consumption increased by more than 1.5 times. This shows that the proposed algorithm is efficient.

5. Conclusions

An adaptive moving mesh method for optimal control problems in viscous incompressible fluid is proposed in this paper, and this is an effective method to solve classical optimal control problems that are constrained by PDEs. The moving distance of the nodes in the proposed strategy is achieved by solving the diffusion equation. An algorithm fully considering the characteristics of the control problem is given.

The fluid states is dominated by the incompressible Navier–Stokes equation in this paper, and thus the proposed method and algorithm can easily generalize to other optimal control problems that are constrained by PDEs. Finally, the numerical examples provided show that the mesh can be concentrated in areas where the solution changes drastically, and the points on the boundary are not forced to remain unchanged.

Author Contributions: Conceptualization, J.L. and H.X.; methodology, X.D.; software, X.D.; validation, J.L., H.X. and X.D.; formal analysis, J.L.; investigation, J.L.; resources, J.L.; data curation, X.D.; writing—original draft preparation, J.L.; writing—review and editing, J.L.; visualization, J.L.; supervision, J.L.; project administration, J.L.; funding acquisition, J.L. All authors have read and agreed to the published version of the manuscript.

Funding: This work was supported by the the Natural Science Foundations of Shaanxi Province of China (2020JM-571, 2021JM1002) and the Science Foundation of the Education Department of Shaanxi Province of China (17JK0344).

Institutional Review Board Statement: Not applicable.

Informed Consent Statement: Not applicable.

Data Availability Statement: Not applicable.

Acknowledgments: The authors would like to thank the referees and the editors for their valuable comments that led to improvements of this work.

Conflicts of Interest: The authors declare no conflict of interest.

References

1. Bonnans, J.F.; Shapiro, A. *Perturbation Analysis of Optimization Problem*; Springer: New York, NY, USA, 2000.
2. Clarke, F.H. *Optimization and Nonsmooth Analysis*; John Wiley Sons: Amsterdam, The Netherlands, 1983.
3. Lions, J.L. *Optinal Control of System Governed by Partial Differential Equations*; Springer: Berlin, Germany, 1971.
4. Hinze, M.; Pinnau, R.; Ulbrich, M.; Ulbrich, S. *Optimization with PDE Constraints*; Springer: Dordrecht, The Netherlands, 2009.
5. Liu, W.B.; Yan, N.N. *Adaptive Finite Elements Methods for Optimal Control Problem Governed by PDEs*; Sciences Press: Beijing, China, 2008.
6. Neittaanmaki, P.; Sprekels, J.; Tiba, D. *Optimization of Elliptic Systems: Theory and Applications*; Springer Science Business Media Inc.: New York, NY, USA, 2006.
7. Tiba, D. *Optimal Control of Nonsmooth Distributed Parameter Systems*; Lecture Notes in Math. 459; Springer: Berlin, Germany, 1990.
8. Jameson, A. Aerodynamic design via control theory. *J. Sci. Comput.* **1998**, *3*, 233–260. [CrossRef]
9. Jameson, A.; Martinelli, L.; Pierce, N.A. Optimum aerodynamic design using the Navier–Stokes equations. *Theor. Comput. Fluid Dyn.* **1998**, *10*, 213–237. [CrossRef]
10. Mackenzie, J.A.; Nolan, M.; Rowlatt, C.F.; Insall, R.H. An adaptive moving mesh method for forced curve shortening flow. *SIAM J. Sci. Comput.* **2019**, *41*, A1170–A1200. [CrossRef]
11. Abergel, F.; Temam, R. On Some Control Problems in Fluid Mechanics. *Theor. Comput. Fluid Dyn.* **1990**, *1*, 303–325. [CrossRef]
12. Barbu, V. Optimal contrtol of Navier–Stokes equations with perioeic inputs. *Nonlinear Anal.* **1998**, *31*, 1531. [CrossRef]
13. De Los Reyes, J.C.; Griesse, R. State-constrained optimal control of the three dimensional stationary Navier–Stokes equations. *J. Math. Anal. Appl.* **2008**, *343*, 257–272. [CrossRef]
14. de los Reyes, J.C.; Troltzsch, F. Optimal control of the stationary Navier–Stokes equations with mixed control-state constraints. *SIAM J. Control Optim.* **2007**, *46*, 604–629. [CrossRef]
15. Gunzburger, M.D. *Flow Control*; Springer: New York, NY, USA, 1995.
16. Casas, E. Error estimates for the numerical approximation of a distributed control prob lem for the steady-state Navier-stokes equations. *SIAM J. Control Optim.* **2007**, *46*, 952–982. [CrossRef]
17. Roul, P. A robust adaptive moving mesh technique for a time-fractional reaction–diffusion model. *Commun. Nonlinear Sci. Numer. Simul.* **2022**, *109*, 106290. [CrossRef]
18. Girault, V.; Raviart, P. *Finite Element Method for Navier–Stokes Equations: Theory and Algorithms*; Springer: Heidelberg, Germany, 1996.
19. Temam, R. *Navier–Stokes Equations and Nonlinear Functional Analysis*; SIAM: Philadelphia, PA, USA, 1983.
20. Liu, W.B.; Yan, N.N. A posteriori error estimates for control problems governed by Stokes equations. *SIAM J. Numer. Anal.* **2003**, *40*, 1850–1869. [CrossRef]
21. Wang, G. Optimal control of 3-dimensional Navier–Stokes equations with state constraints. *SIAM J. Control Optim.* **2002**, *41*, 583–606. [CrossRef]
22. Li, R.; Liu, W.B.; Ma, H.; Tang, T. Adaptive finite element approximation of elliptic optimal control. *SIAM J. Control Optim.* **2002**, *41*, 1321–1349. [CrossRef]

23. Kurganov, A.; Qu, Z.; Rozanova, O.S.; Wu, T. Adaptive Moving Mesh Central-Upwind Schemes for Hyperbolic System of PDEs: Applications to Compressible Euler Equations and Granular Hydrodynamics. *Commun. Appl. Math. Comput.* **2021**, *3*, 445–480. [CrossRef]
24. Duan J.M.; Tang, H.Z. High-order accurate entropy stable adaptive moving mesh finite difference schemes for special relativistic (magneto)hydrodynamics. *J. Comput. Phys.* **2022**, *456*, 111038. [CrossRef]
25. Almatrafi, M.B.; Alharbi, A.; Lotfy, K.; El-Bary, A.A. Exact and numerical solutions for the GBBM equation using an adaptive moving mesh method. *Alex. Eng. J.* **2021**, *60*, 4441–4450. [CrossRef]
26. Babuska, I.; Rheinboldt, W.C. Error estimates for adaptive finite element computations. *SIAM J. Numer. Anal.* **1978**, *15*, 736–754. [CrossRef]
27. Oden, J.T.; Wu, W.; Ainsworth, M. An a posteriori error estimate for finite element approximations of the Navier-stokes equations. *Comput. Methods Appl. Mech. Eng.* **1993**, *111*, 185–202. [CrossRef]
28. Verfurth, R. *A Review of A Posteriori Error Estimation and Adaptive Mesh-Refinement Techniques*; Wiley: Hoboken, NJ, USA, 1996.
29. Verfurth, R. A posteriori error estimators for the Stokes equations. *Numer. Math.* **1989**, *55*, 309–325. [CrossRef]
30. Luo, D.; Huang, W.; Qiu, J. A quasi-lagrangian moving mesh discontinuous galerkin method for hyperbolic conservation laws. *J. Comput. Phys.* **2019**, *396*, 544–578. [CrossRef]
31. Hubbard, M.E.; Ricchiuto, M.; Sarmany, D. Space-time residual distribution on moving meshes. *Comput. Math. Appl.* **2020**, *79*, 1561–1589. [CrossRef]
32. Bagherpoorfard, M.; Soheili, A.R. Moving mesh version of wave propagation algorithm based on augmented riemann solver. *Appl. Math. Comput.* **2020**, *375*, 125087–125103. [CrossRef]
33. Ainsworth, M.; Oden, J.T. *A Posteriori Error Estimation in Finite Element Analysis*; Pure and Applied Mathematics; Wiley-Interscience: Hoboken, NJ, USA, 2000.
34. Koncz, V.; Izsák, F.; Noszticzius, Z.; Kály-Kullai, K. Adaptive moving mesh algorithm based on local reaction rate. *Heliyon* **2021**, *7*, e05842. [CrossRef] [PubMed]
35. Tang, T. Moving mesh methods for computational fluid dynamics. *Contemp. Math.* **2004**, *383*, 141–173.
36. Mackenzie, J.A.; Mekwi, W.R. On the Use of Moving Mesh Methods to Solve PDEs. In *Adaptive Computations: Theory and Algorithms*; Tang, T., Xu, J., Eds.; Science Press: Beijing, China, 2007.
37. Ceniceros, H.D.; Hou, T.Y. An efficient dynamically adaptive mesh for potentially singular solutions. *J. Comput. Phys.* **2001**, *172*, 609–639. [CrossRef]
38. Huang, W.; Zhan, X. Adaptive moving mesh modeling for two dimensional groundwater flow and transport. In *Recent Advances in Adaptive Computation, Contemporary Mathematics*; AMS: Providence, RI, USA, 2004; Volume 383, pp. 283–296.
39. Budd, C.J.; Williams, J.F. Parabolic Monge-Ampere methods for blow-up problems in several spatial dimensions. *J. Phys. A* **2006**, *39*, 5425–5444. [CrossRef]
40. Zegeling, P.A.; Kok, H.P. Adaptive moving mesh computations for reaction-diffusion systems. *J. Comput. Appl. Math.* **2004**, *168*, 519–528. [CrossRef]
41. Duan, X.; Cao, Q.; Tan, H. A new moving mesh method for solving the two-dimensional Navier–Stokes equation. *Chin. J. Eng. Math.* **2019**, *36*, 431–438.
42. Di, Y.; Li, R.; Tang, T.; Zhang, P. Moving Mesh Finite Element Methods for the Incompressible Navier–Stokes Equations. *SIAM J. Sci. Comput.* **2016**, *26*, 1036–1056. [CrossRef]
43. Song, L.; Su, H.; Feng, X. Recovery-based error estimatorfor stabilized finite element method for the stationary Navier–Stokes problem. *SIAM J. Sci. Comput.* **2016**, *38*, A3758–A3772. [CrossRef]
44. Zhang, T.; Li, S. A posteriori error estimates of finite element method for the time-dependent navier-stokes equations. *Appl. Math. Comput.* **2017**, *315*, 13–26. [CrossRef]